

# *In silico* evaluation of potential murine M49 DNA aptamer on ORF7a of SARS-COV-2: A similar target

Nor Azlina AHMAD <sup>1</sup> , Razauden Mohamed ZULKIFLI <sup>1,5\*</sup> , Huszalina HUSSIN <sup>1</sup> , Syazwani Itri AMRAN <sup>1</sup> , Muhammad Helmi NADRI <sup>2</sup> , Saiful Izwan ABDUL RAZAK <sup>3</sup> , Sabrinah ADAM <sup>4</sup> , Farahwahida MOHD YUSOF <sup>5</sup> 

<sup>1</sup> Department of Biosciences, Faculty of Science, Universiti Teknologi Malaysia, Johor Bahru, Malaysia.

<sup>2</sup> Innovation Centre in Agritechology for Advanced Bioprocessing, Universiti Teknologi Malaysia, 84600 Pagoh, Johor, Malaysia.

<sup>3</sup> School of Biomedical Engineering and Health Sciences, Faculty of Engineering, University Teknologi Malaysia, Johor Bahru, Malaysia

<sup>4</sup> Azman Hashim International Business School, Universiti Teknologi Malaysia, Johor Bahru, Malaysia.

<sup>5</sup>Centre of Research for Fiqh Science and Technology (CFIRST), Universiti Teknologi Malaysia, Johor Bahru, Malaysia.

\* Corresponding Author. E-mail: [razauden@fbb.utm.my](mailto:razauden@fbb.utm.my) (R.M.Z.); Tel. +607-5631357.

Received: 23 January 2022 / Revised: 02 June 2022 / Accepted: 20 June 2022

**ABSTRACT:** DNA aptamers are short nucleotides with a high affinity for their target. However, the process of isolating aptamers via the systematic evolution of ligands by exponential enrichment (SELEX) procedure is laborious. Therefore, an *in silico* approach is used to screen potential DNA aptamer candidates as a kickstart specifically for ORF7a of SARS-COV-2. By applying the TM-align program, the murine receptor (CD200R) protein was found to have structural similarities with ORF7a. Based on the literature, this CD200R protein is successfully bound by M49 DNA aptamers experimentally. Herein, the 3D structure of the M49 DNA aptamer was generated using Mfold, RNA Composer webserver, Discovery Studio Visualizer, and UCSF Chimera software, and the docking simulation was predicted using the HDock webserver. The binding energy scores for the M49-CD200R complex were slightly higher than those for the M49-ORF7a complex with -233.78 and -220.11, respectively. The molecular interaction in the complexes was contributed by the hydrogen bond. In conclusion, the M49 aptamer of CD200R protein can bind to the other similar target, the ORF7a protein of SARS-COV-2. Even though CD200R and ORF7a proteins share structural similarities, the binding sites of the individual complex are distinct. The current study shows that two different proteins with structural similarities may have a possibility to share the same DNA aptamer. This strategy may result in efficient aptamer discovery using an *in silico* method as a first step.

**KEYWORDS:** SARS-COV-2; ORF7a; DNA aptamer; molecular docking

## 1. INTRODUCTION

The report on the new coronavirus infectious disease was firstly claimed in December 2019 in Wuhan, China. Most of the patients were diagnosed with severe pneumonia together with common symptoms such as fever, cough, shortness of breath, and fatigue [1]. This infectious disease is also known as COVID-19 which is caused by severe acute respiratory syndrome (SARS-COV-2). To date, World Health Organization (WHO) reported about 150 million confirmed cases with 3 millions of fatality (<https://covid19.who.int/>). The number of infected and death cases is still on arising.

SARS-COV-2 belongs to the betacoronavirus family Coronaviridae and has high nucleotide sequence similarity with severe acute respiratory syndrome (SARS) and Middle East coronavirus (MERS) with 79.5% and 50% similarity, respectively [2]. Therefore, protein exploration in SARS-COV-2 is frequently discussed and compared with SARS-COV. This virus contains a positive single-stranded RNA (+ssRNA virus) encoding four structural proteins (spike (S), nucleocapsid (N), membrane (M) and envelope (E) proteins) and six accessory proteins (ORF3a, ORF6, ORF7a, ORF7b, ORF8a, ORF8b) with a length of about 30 kilobases [3].

Based on the structural orientation of SARS, the S, E, M, ORF3a, ORF3b, ORF7a, ORF7b, ORF8a, and ORF14 are known to be surface proteins (SPs) [4]. It can be assumed that the surface proteins (SPs) of SARS-

**How to cite this article:** Ahmad NA, Mohamed Zulkifli R, Hussin H, Amran SI, Nadri MH, Abdul Razak SI, Adam S, Mohd Yusof F. *In silico* Evaluation of Potential Murine M49 DNA aptamer on ORF7a of SARS-COV-2. J Res Pharm. 2023; 27(1): 232-240.

COV-2 are distributed in this region. The function of these SPs varies depending on their location inside or outside the virion. A previous study has shown that S, E, M of SARS-COV is essential for the attachment of the virus to the host cell and is considered an attractive target for targeting SARS-COV-2 [5]-[7]. However, information about accessory proteins, especially ORF7a as a recognition element, is poorly known. Understanding the structural ability of this protein will facilitate alternative diagnostic targets against SARS-COV-2.

The crystal structure of ORF7a from SARS-COV-2 has been identified and deposited in Protein Data Bank (PDB) (PDB ID: 6W37). It possesses type 1 transmembrane protein with 121 amino acids in length. The sequence similarity of SARS-COV-2 as compared to SARS is 85.2% and 95.9%, respectively [3]. The presence of ORF7a on the surface of the virus provides an alternative target for virus identification, especially for diagnostic assays.

Recently, the development of nucleic acid aptamers capable of specifically interacting with viruses has been intensively investigated [8]-[10]. Aptamers are short single-stranded oligonucleotides (RNA or DNA) and are classified as a type of "chemical antibody" in a wide range of applications [11]. Aptamers can be obtained and selected from a random oligonucleotide library by the systematic evolution of ligands using the exponential enrichment (SELEX) technique [12]. Such aptamers can be used for specific recognition of infectious agents and can also knock down their functions [13]. The interaction between the aptamer and viral proteins is influenced by the folding of the aptamer, especially by three-dimensional (3-D) structures that contribute to the formation of hydrogen bonds, van der Waals interactions, and electrostatic activities [14].

Computational biology is now routinely used to discover potential candidates for new drugs using target structure data. This is due to the need for time and cost-efficient techniques to determine lead structures [15]. Using a similar approach, this study aims to investigate the interaction of the DNA aptamer of ORF7a protein of SARS-COV-2 using a series of computational methods. Primarily, the structural similarity search was performed using TM-align web server to identify proteins that have similar structures to ORF7a and have DNA aptamer in the literature. The obtained aptamer was further evaluated for its ability to interact with ORF7a protein using molecular docking simulation.

Translated with [www.DeepL.com/Translator](http://www.DeepL.com/Translator) (free version)

## 2. RESULTS AND DISCUSSION

### 2.1 Structural similarity of ORF7a of SARS-COV-2

TM-align is the algorithm to identify the best structural alignment between two different proteins [16], [17]. Based on TM-align output, the structure of ORF7a protein have similarity to the extracellular portion of mouse CD200R (PDB ID: 4BFG) with TM-score and RMSD values of 0.73 and 2.15, respectively. CD200 is a commonly distributed membrane glycoprotein that regulates myeloid cell activity through its interaction with an inhibitory receptor (CD200R) [18]. The receptor, CD200R1 is a glycoprotein type I that functioned in delivering the immune inhibitory signal to CD200. It holds a transmembrane region, two Ig-like domains, and a cytoplasmic tail containing an NXPY motif [19]. Herein, most of the aligned residues between ORF7a (PDB ID: 6W37) and mouse CD200R protein (PDB ID: 4BFG) are located at the N-terminal of both proteins (Figure 1). This protein was further investigated for any aptamer-related studies in the literature, and the best aptamer against this protein was identified as M49. The aptamer possesses 25 nucleotides at a random region and flanked 25-mer of primer binding regions at 5' and 3' which is isolated from 15 rounds of SELEX procedure [19].

### 2.2 Structural validation of CD200R and ORF7a of SARS-COV-2

The quality of both CD200R and ORF7a proteins was analyzed using PROCHECK and ProSA (Protein Structure Analysis) webservers. The Ramachandran plots for the proteins are presented in Figure 2. The CD200R and ORF7a proteins displayed 92.3% and 80.4% residues in the favored region, respectively with no residue in the disallowed region (Figure 2). Next, the ProSA assessment is used to validate protein structures obtained from X-ray analysis, NMR spectroscopy, and theoretical calculations [20]. The overall protein structure quality for CD200R and ORF7a proteins was found to be in good model quality of Z-score at -5.96 and -3.09, respectively. This plot is useful to examine whether the z-score of the CD200R and ORF7a proteins are within the range of scores normally observed for proteins of similar size belonging to one of these groups.

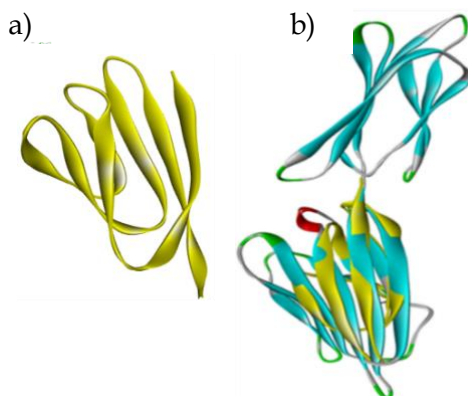


**Figure 1:** (a) 3D structure of ORF7a protein of SARS-COV-2 (PDB ID: 6W37). (b) The superimposition of ORF7a of SARS-COV-2 (PDB ID:6W37) (yellow) and the extracellular portion of mouse CD200R (PDB ID: 4BFG) (cyan).

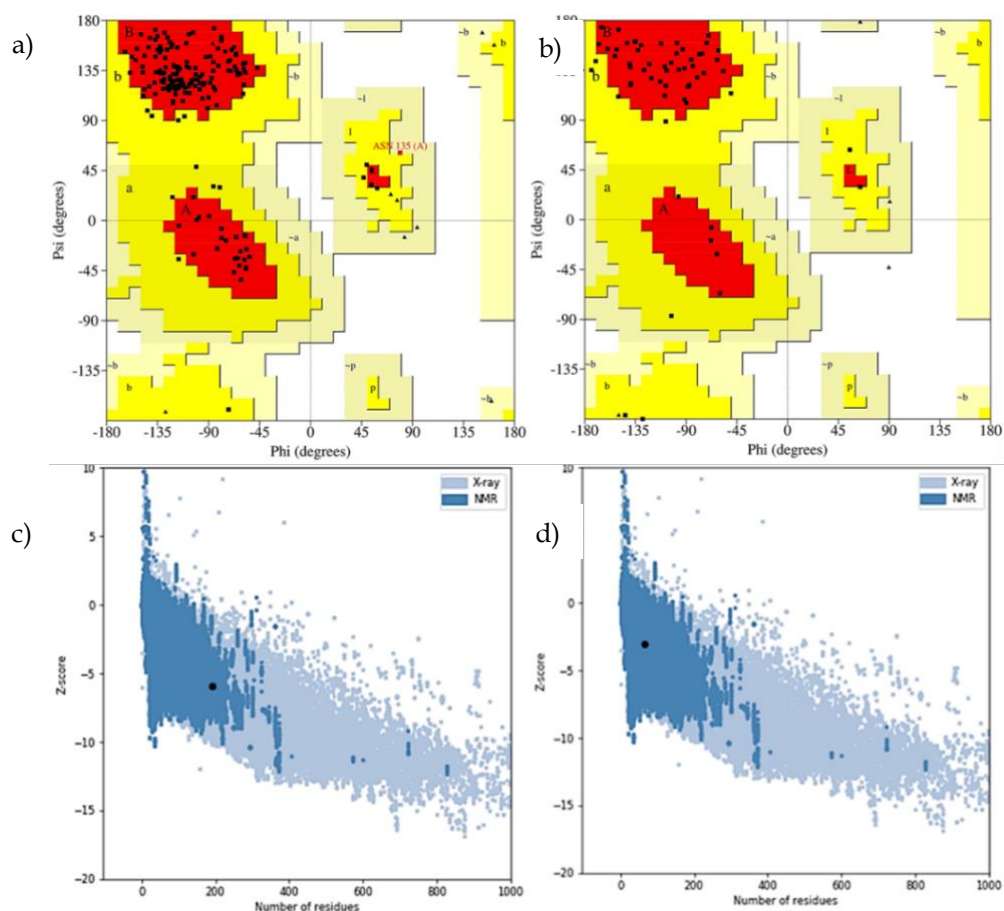


**Figure 2:** Ramachandran plot assessment generated using PROCHECK web server of CD200R (a) and ORF7a of SARS-COV-2 (b) depicting 92.3% and 80.4% residues in the favored region, respectively. ProSA assessment of CD200R (c) and ORF7a of SARS-COV-2 (d) indicate both structures reside in the range of scores similar to native structures derived from NMR and X-ray.

### 2.3 3D structure of M49 aptamer

The secondary structure of M49 was modeled by the MFold web server based on the primary sequence from the original paper [19]. The obtained aptamers possess DNA type-B conformation of the Watson-Crick

base pairing model. M49 contains three sets of conformation at Stem I (G1-T12), Stem II (A14-C18), and Stem III (A21-G26) with the presence of 2 small bulges and two loops. The modeled 3D structure was further optimized to achieve thermodynamically stable after being generated using the RNAComposer webserver (Figure 3). The structure generated was saved as .pdb files for molecular interaction analysis via docking simulation.

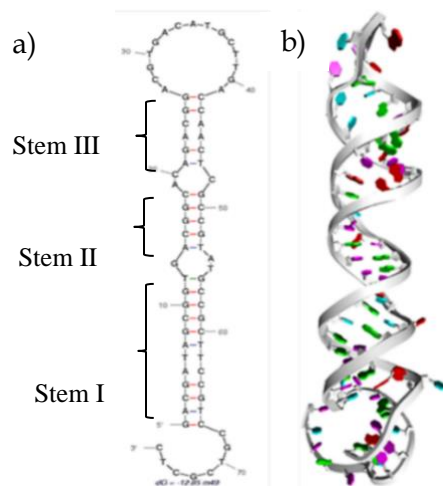


**Figure 3:** The (a) 2-D and (b) 3-D structure prediction of M49 DNA aptamers.

#### 2.4 Molecular docking simulation of M49 aptamer with CD200R

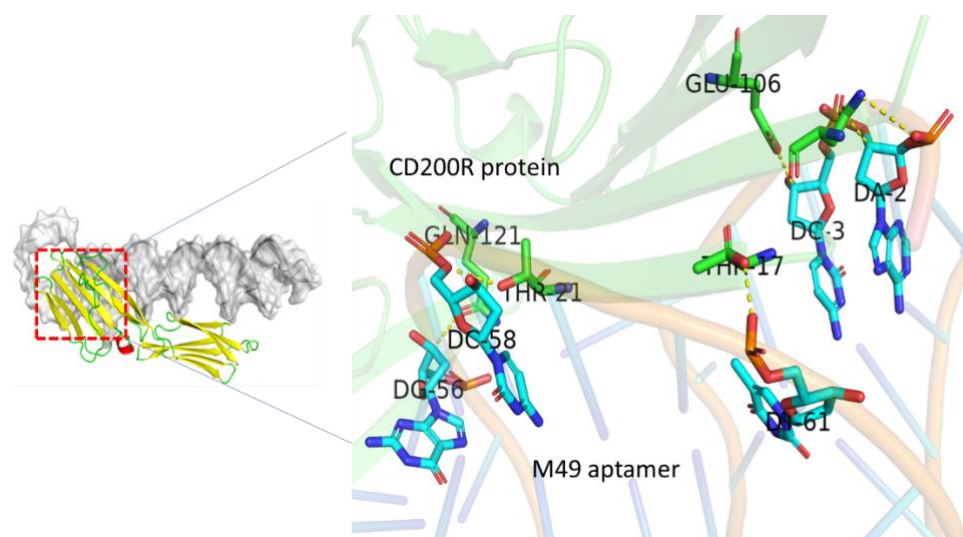
We performed the computational DNA-protein docking approach to analyze structural complexes of the M49 aptamer with CD200R protein. The intermolecular interaction analysis of the M49-CD200R complex was performed using HDOCK [21] (<http://HDOCK.phys.hust.edu.cn/>). The results indicated that the M49-CD200R complex holds a docking energy score of -233.78. 100 poses were generated, and the highest binding energy score was considered the best fit for the M49-CD200R complex.

Table 1 shows the docking output of the complex, including parameters such as interacting residues, distance, and interaction type. Most of the interactions were contributed by hydrogen bonding at THR17, THR21, GLU106, ASN113, and LYS116. The THR17 possesses a preference for thymine from the aptamer region due to the methyl-methyl contact. The ASN113 demonstrates typical amino acid-base pair when interacting with adenine [22] to produce a hydrogen bond. The interacting residue of THR17, ASN113, and LYS116 act as a donor to the phosphate backbone of DNA.

Besides hydrogen bonding, salt bridge interaction was reported between the LYS116 of CD200R and G59 of the M49 aptamer. Lysine's side-chains play a vital role in protein-DNA recognition especially in the formation of salt bridges with the negatively charged oxygen-phosphate groups [23].

**Table 1:** Docking simulation results and the interaction type between CD200R protein and M49 aptamer.

Interacting residue:nucleotide	Distance (Å)	Interaction type	Donor	Acceptor
THR17:DT61	2.29888	Hydrogen Bond	THR17:OG1	DT61:OP2
ASN113: DA2	2.95726	Hydrogen Bond	DA2:C3'	ASN113:OD1
GLU106: DC3	2.86828	Hydrogen Bond	DC3:C3'	GLU106:OE2
THR21:DC58	3.28354	Hydrogen Bond	THR21:OG1	DC58:O5'
GLN121: DG56	3.18702	Hydrogen Bond	DG56:C3'	GLN121:OE1
ASN113:DA2	3.38223	Hydrogen Bond	ASN113:ND2	DA2:OP2
LYS116:DG59	3.68838	Hydrogen Bond; Electrostatic; Salt bridge	LYS116:NZ	DG59:OP2
THR21: DC58	3.54888	Hydrogen Bond	DC58:C6	THR21:OG1
LYS51:DA5	4.43041	Electrostatic	LYS51:NZ	DA5:OP2



**Figure 4:** The overall structures of the CD200R (yellow) and M49 aptamer (grey). The enlarged figure (right) shows the hydrogen bond interactions observed at Thr17, Thr21, Glu106, and Gln121 of CD200R (green) and DA2, DC3, DG56, and DC58 of M49 aptamer (cyan).

## 2.5 Molecular docking simulation of M49 aptamer with ORF7a

The intermolecular interaction analysis of the M49-ORF7a complex was performed using HDOCK. The docking energy score of the M49-ORF7a aptamer-protein complex is -220.11 with the presence of hydrogen bonding and electrostatic interaction. The ORF7a protein-interacting side contains polar amino acids such as THR3, TYR5, GLN6, ASN28, THR46, GLN47, and GLN61. They are important for hydrogen bonding formation with the M49 aptamer at stems I and II containing DG11, DT12, DC50, DG52, and DT53.

Lysine and arginine side chains are important in nucleotide binding, either via hydrogen bond formation or electrostatic interactions [23], as demonstrated by ARG63, ARG65, and LYS57 of ORF7a protein. In the protein-DNA interaction, hydrogen bonds demonstrate the strongest specificity [24].

**Table 2:** Docking simulation results and the interaction type between ORF7a protein and M49 aptamer.

Interacting residue:nucleotide	Distance (Å)	Interaction type	Donor	Acceptor
THR46 : DG11	2.26934	Hydrogen Bond	THR46:OG1	DG11:OP2
TYR3 : DT53	2.66322	Hydrogen Bond	TYR3:N	DT53:OP2
ASN28: DG11	2.62226	Hydrogen Bond	ASN28:ND2	DG11:OP2
GLN61 : DT12	2.88731	Hydrogen Bond	GLN61:NE2	DT12:O4
GLN47: DT12	3.30172	Hydrogen Bond	GLN47:NE2	DT12:O4
TYR5 : DG52	3.2651	Hydrogen Bond	TYR5:N	DG52:N7
GLN6: DC50	3.30312	Hydrogen Bond	GLN6:NE2	DC50:O5'
LYS57:DC9	3.17472	Hydrogen Bond;	LYS57:NZ	DC9:OP2
ARG63:DG13	3.79268	Electrostatic; Salt	ARG63:NH1	DG13:OP2
ARG65:DG49	3.39068	bridge	ARG65:NH2	DG49:OP2
ARG10:DT12	4.5608	Electrostatic	ARG10:NH1	DT12:OP2

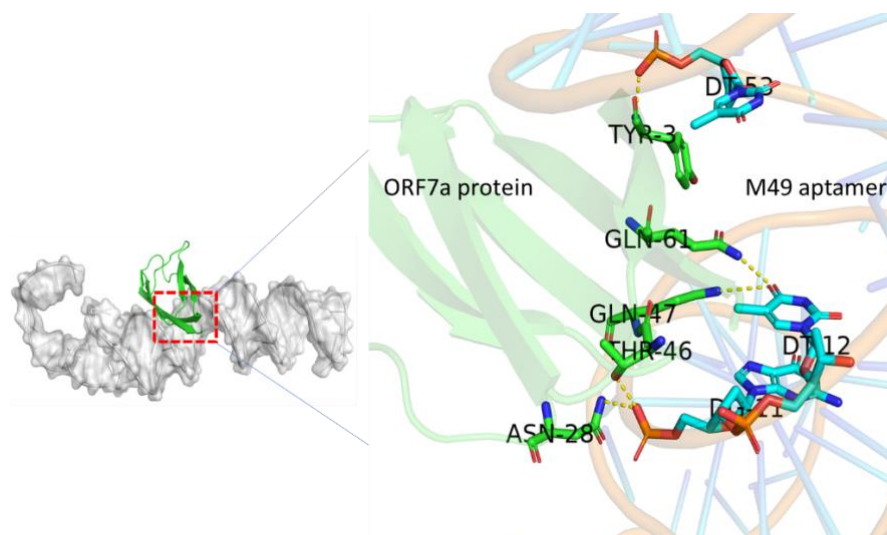


**Figure 5:** The ORF7a (green)- M49 aptamer (grey) complex. The enlarged figure (right) shows hydrogen bond interactions were observed at Thr3, Asn28, Glu61, and Thr46 of ORF7a protein of SARS-COV-2 (green) and DT11, DT12, and DT53 of M49 aptamer (cyan).

The HDOCK docking energy score is negatively correlated with the binding energy. A negative value shows a spontaneous reaction between aptamer with the protein complex. Thus, the M49-CD200R aptamer-protein complex has a higher binding affinity than the M49-ORF7a aptamer-protein complex. This is due to the presence of multiple hydrogen bonding in the M49-CD200R complex as compared to the M49-ORF7a complex and the addition of salt bridges and charges amino acids residue.

The present study focuses on the potential of structural similarity of two different proteins that bind to the same aptamer. It was observed that the binding sites of the proteins were different albeit sharing a similar structure. This suggested that the factor for aptamer and target ligand interaction is not solely on the higher similarity of the two proteins as a whole but also multifactorial such as the folding, the exposure, and the sequence of the binding region.

Besides this finding, the interacting hydrogen bonds in ORF7a of SARS-COV-2 mentioned previously are conserved in the ORF7a of the SARS-COV. This is because the conservation of base-contacting positions is dependent on the family's binding class [24]. In this case, the ORF7a-contacting positions between SARS-COV-2 and SARS-COV are highly specific, and the M49 aptamer may be able to interact with the ORF7a protein of SARS-COV.

### 3. CONCLUSION

In conclusion, the *in silico* study demonstrated the ability of M49 aptamer to bind to the ORF7a protein of SARS-COV-2. The hydrogen bond is the dominant interaction for the formation of both M49-CD200R and M49-ORF7a complexes. M49 interacts with different amino acids from different binding regions of both CDR200 and ORF7a, suggesting the structural similarity of a protein is not the main factor for the aptamer binding site but more on the suitability of the remote region. In the future, more research on optimization of the M49 aptamer against ORF7a protein is necessary, such as rational truncation or mutagenesis, to enhance its specificity using an *in silico* approach.

### 4. MATERIALS AND METHODS

#### 4.1 Structural similarity of ORF7a of SARS-COV-2

The sequence and 3D structure of ORF7a were retrieved from UniProt (UniProtKB: P0DTC7) and Protein Data Bank (PDB ID: 6W37), respectively. The protein structural alignment of ORF7a was performed using the mTM-align webserver (Dong et al., 2018). This server offers fast protein structure database search and multiple protein structure alignment. The input file format was .pdb or mmCIF. The list of proteins obtained from the output was filtered based on their availability of aptamer from a previous study. In this study, the protein with high similarity with ORF7a is murine CD200R which possesses a DNA aptamer named M49.

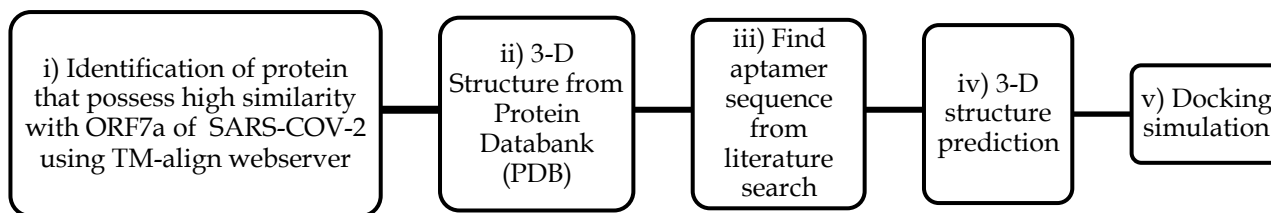


**Figure 6:** Workflow was used in this study. It consists of five main steps, involving identifying the protein with high similarity with ORF7a protein of SARS-COV-2 using TM-align (step 1), assessing the 3-D structure of the resulting protein in Protein Databank (step 2), finding the aptamer sequence of resulting protein from the literature search (step 3), constructing the 3-D structure of aptamer *in silico* (step 4) and molecular docking simulation (step 5).

#### 4.2 3D structure preparation of ORF7a and its validation

The crystal structure of ORF7a was obtained from RCSB PDB (PDB ID:6W37). Further, the ORF7a model was then subjected to stereochemical validation using PROCHECK and PROSA Web server (<https://prosa.services.came.sbg.ac.at/prosa.php>) were employed to select a high-quality model for docking studies. Ramachandran plot was generated for the model to visualize energetically allowed regions for backbone  $\psi$  (psi) and  $\phi$  (phi) dihedral angles of amino acid residues.

#### 4.3 3D structure preparation of M49 DNA aptamer

In this study, the primary sequence of M49 aptamer (5'-GACGATAGCGGTGACGGCACAGACGGACGTGACATGCTTGACCAACTCGCCGATGCCGCTTCCGTCCGTCGCTC-3') was obtained from Prodeus *et al.*, 2014 [19]. The sequence M49 was further examined using MFold web server [25] for linear ssDNA secondary folding structure prediction and hybridization. The input (dot-bracket format) obtained from Mfold was further investigated using RNA Composer (<http://rnacomposer.ibch.poznan.pl/Home>). As the algorithm of this software is in RNA form, thymine (T) in the DNA sequence was replaced with uracil (U) automatically. Therefore, the modifications of uracil to thymine and sugar ribose to deoxyribose were performed using Discovery Studio Visualizer (DSV) software (Windows version 2017 R2 V17.0.16349). After both steps of modifications, ssDNA was constructed, and the structure were energy minimized using UCSF Chimera 1.13 [26]. The structural prediction pipeline used in this manuscript has been validated (data not shown) by comparing the Root Mean Square Deviation (RMSD) value with the hairpin structure deposited in PDB. The optimized structure was saved in .pdb file format for docking analysis.

#### 4.4 Molecular docking simulation

To identify the binding pattern of the M49 aptamer and ORF7a model, we performed the molecular docking simulation using HDOCK. The obtained PDB files of the proteins and M49 aptamer were used as the input receptor and ligand molecule, respectively, in HDOCK [21]. As the binding sites of ORF7a are unknown, blind docking was first performed. The scoring energy produced from HDOCK was used to analyze the possible binding site between M49 aptamer and ORF7a. The intermolecular interaction in the complex was visualized using PyMol and DSV.

**Acknowledgments:** This study was supported by PRGS: ICC (PY/2020/03762).

**Author contributions:** Concept - R.M.Z, H.H, S.I.A, N.A.A; Design - R.M.Z, H.H, S.I.A., S.I.A.R, S.A; Supervision - R.M.Z.; Resources - R.M.Z.; Materials - N.A.A; Data Collection and/or Processing - N.A.A.; Analysis and/or Interpretation - N.A.A., H.H, S.I.A.; Literature Search - N.A.A.; Writing - N.A.A.; Critical Reviews - R.M.Z, M.H.N, H.H

**Conflict of interest statement:** The authors declared no conflicts of interest.

## REFERENCES

- [1] Pedersen SF, Ho YC. SARS-CoV-2: A storm is raging. *J. Clin. Invest.* 2020; 130(5): 2202–2205. [\[CrossRef\]](#)
- [2] Koyama T, Platt D, Parida L. Variant analysis of SARS-CoV-2 genomes. *Bull World Heal. Organ.* 2020; 98: 495–504. [\[CrossRef\]](#)
- [3] Yoshimoto FK. The Proteins of Severe Acute Respiratory Syndrome Coronavirus-2 (SARS CoV-2 or n-COV19), the Cause of COVID-19. *Protein J.* 2020 ; 39 (3): 198–216. [\[CrossRef\]](#)
- [4] Roper RL, Rehm KE. SARS vaccines: Where are we?. *Expert Rev. Vaccines.* 2009; 8 (7): 887–898. [\[CrossRef\]](#)
- [5] Ou X, Liu Y, Lei X, Li P, Mi D, Ren L, Guo L, Guo R, Chen T, Hu J, Xiang Z, Mu Z, Chen X, Chen J, Hu K, Jin Q, Wang J, Qian Z. Characterization of spike glycoprotein of SARS-CoV-2 on virus entry and its immune cross-reactivity with SARS-CoV. *Nat. Commun.* 2020; 11 (1): 1620. [\[CrossRef\]](#)
- [6] Song Y, Song J, Wei X, Huang M, Sun M, Zhu L, Lin B, Shen H, Zhu Z, Yang C. Discovery of Aptamers Targeting Receptor-Binding Domain of the SARS-CoV-2 Spike Glycoprotein. *Anal. Chem.* 2020; 92 (14), 9895–9900. [\[CrossRef\]](#)
- [7] Bianchi M, Benvenuto D, Giovanetti M, Angeletti S, Ciccozzi M, Pascarella S. SARS-COV-2 Envelope and Membrane Proteins: Structural Differences Linked to Virus Characteristics?. *Biomed Res. Int.* 2020: 1–6. [\[CrossRef\]](#)
- [8] Bala J, Chinnapaiyan S, Dutta RK, Unwalla H. Aptamers in HIV research diagnosis and therapy. *RNA Biol.* 2018; 15 (3): 327–337. [\[CrossRef\]](#)
- [9] Yu X, Wang Y, Yang H, Huang X. Prediction of the binding affinity of aptamers against the influenza virus. *SAR QSAR Environ. Res.* 2019; 30 (1): 51–62. [\[CrossRef\]](#)
- [10] Chathappady House NN, Palissery S, Sebastian H. Corona Viruses: A Review on SARS, MERS and COVID-19. *Microbiol. Insights.* 2021(14): 1–8 [\[CrossRef\]](#).
- [11] Zhu C, Li L, Fang S, Zhao Y, Zhao L, Yang G, Qua F. Selection and characterization of an ssDNA aptamer against thyroglobulin. *Talanta.* 2021; 223 (P1): 121690. [\[CrossRef\]](#)
- [12] Tuerk C, Gold L. Systematic evolution of ligands by exponential enrichment: Systematic Evolution of Ligands by Exponential Enrichment: RNA Ligands to Bacteriophage T4 DNA Polymerase. *Science* (80). 1990; 249 (4968): 505–510. [\[CrossRef\]](#)
- [13] Davydova A, Vorobjeva M, Pyshnyi D, Altman S, Vlassov V, Venyaminova A. Aptamers against pathogenic microorganisms. *Crit. Rev. Microbiol.* 2016; 42 (6): 847–865. [\[CrossRef\]](#)
- [14] Hu B, Zhou R, Li Z, Ouyang S, Li Z, Hu W, Wang L, Jiao B. Study of the binding mechanism of aptamer to palytoxin by docking and molecular simulation. *Sci. Rep.* 2019; 9 (1): 1–11. [\[CrossRef\]](#)
- [15] Bini A, Mascini M, Mascini M, Turner APF. Selection of thrombin-binding aptamers by using computational approach for aptasensor application. *Biosens. Bioelectron.* 2011; 26 (11): 4411–4416. [\[CrossRef\]](#)
- [16] Zhang Y, Skolnick J. TM-align: A protein structure alignment algorithm based on the TM-score. *Nucleic Acids Res.* 2005; 33 (7): 2302–2309. [\[CrossRef\]](#).
- [17] Dong R, Pan S, Peng Z, Zhang Y, Yang J. MTM-align: A server for fast protein structure database search and multiple protein structure alignment. *Nucleic Acids Res.* 2018; 46 (W1): W380–W386. [\[CrossRef\]](#)
- [18] Hatherley D, Lea SM, Johnson S, Barclay AN. Structures of CD200/CD200 receptor family and implications for topology, regulation, and evolution. *Structure.* 2013; 21 (5): 820–832. [\[CrossRef\]](#)
- [19] Prodeus A, Cydzik M, Abdul-Wahid A, Huang E, Khatri I, Gorczynski R, Gariép J. Agonistic CD200R1 DNA aptamers are potent immunosuppressants that prolong allogeneic skin graft survival. *Mol. Ther. Nucleic Acids* 2014; 3: 1–8. [\[CrossRef\]](#).
- [20] Wiederstein M, Sippl MJ. ProSA-web: Interactive web service for the recognition of errors in three-dimensional

- structures of proteins. *Nucleic Acids Res.* 2007; 35 (2): 407–410. [\[CrossRef\]](#).
- [21] Yan Y, Zhang D, Zhou P, Li B, Huang SY. HDock: A web server for protein-protein and protein-DNA/RNA docking based on a hybrid strategy. *Nucleic Acids Res.* 2017; 45 (W1): W365–W373. [\[CrossRef\]](#).
- [22] Luscombe NM, Laskowski RA, Thornton JM. Amino acid-base interactions: A three-dimensional analysis of protein-DNA interactions at an atomic level. *Nucleic Acids Res.* 2001; 29 (13): 2860–2874. [\[CrossRef\]](#)
- [23] Lacabanne D, Boudet J, Malär AA, Wu P, Cadalbert R, Salmon L, Allain FHT, Meier BH, Wiegand T. Protein Side-Chain-DNA Contacts Probed by Fast Magic-Angle Spinning NMR. *J. Phys. Chem. B.* 2020 ; 124 (49) : 11089–11097. [\[CrossRef\]](#)
- [24] Luscombe NM, Thornton JM. Protein-DNA interactions: Amino acid conservation and the effects of mutations on binding specificity. *J. Mol. Biol.* (2002); 320 (5): 991–1009. [\[CrossRef\]](#)
- [25] Zuker M. Mfold web server for nucleic acid folding and hybridization prediction. *Nucleic Acids Res.* 2003; 31 (13): 3406–3415. [\[CrossRef\]](#).
- [26] Pettersen EF, Goddard TD, Huang CC, Couch GS, Greenblatt DM, Meng EC, Ferrin TE. UCSF Chimera - A visualization system for exploratory research and analysis. *J. Comput. Chem.* 2004; 25 (13): 1605–1612.

This is an open access article which is publicly available on our journal's website under Institutional Repository at <http://dSPACE.marmara.edu.tr>.